Modeling Transfer of electrons between Energy States of an Electrolyte and CdS thin films using Gerischer Model

Article *in* International Journal of Asian Studies · January 2016

CITATIONS
0

READS
45

1 author:

Cliff Orori Mosiori
Technical University of Mombasa
57 PUBLICATIONS **36** CITATIONS

SEE PROFILE

Journal of Scientific Research and Studies Vol. 2(x), pp. xxx-xxx, December, 2015
ISSN 2375-8791

http://www.modernrespub.org/jsrs/index.htm

Full Length Research Paper

Modeling transfer of electrons between energy states of an electrolyte and CdS thin films using Gerischer Model

MOSIORI Cliff Orori[1]*, MAERA John[2], NJOROGE W. Kamande[3], SHIKAMBE T. Reuben[3], MUNJI Matthew [3] and MAGARE Robert[2]

[1]Department of Mathematics and Physical Sciences, Technical University of Mombasa, Box 90420 – 80100 Mombasa, Kenya.
[2]Department of Mathematics and Physical Sciences, Maasai Mara University, Box 861 - 20500, Narok, Kenya.
[3]Department of Physics, Kenyatta University, Box 43844 - 00100, Nairobi, Kenya.

*Corresponding author. E-mail: cliffmosiori@gmail.com

Accepted 18 December, 2015

A number of models have been developed to describe electron transfer between electrolytes and group II–VI binary semiconductors. In this report, a study was conducted to describe and model electron transfer between an inorganic semiconductor, (i.e. CdS) and a ferric oxidizing/reducing agent [i.e. $K_3Fe(CN)_6/K_4Fe(CN)_6$]. The study describes the interfacial electron transfer using the semi-classical theory approaches as described by Marcus and later developed by Gerischer and therefore called Gerischer model as it is applied to heterogeneous electron transfer in a semiconductor - electrolyte interface. CdS thin films were grown by electro-deposition method on the indium tin oxide (ITO) substrates and were used as electrodes. The data collected was used to determine the kinetic constant rates and re-orientation energies as measured in the solutions with different concentration of redox system, Fe^{+3}/ Fe^{+2}. Experiments showed that when concentration of oxidized species increased and causing an increase in $E^{\circ}_{F,redox}{}^{2}$ activity, the kinetic constant rates decreases inversely. Equally light induced current at 0.0V/Ag was higher when the ratio of the oxidant-reductant (i.e. 2/0.02 and 0.2/0.02) was high. EIS studies revealed that for the two ratios of. 2/0.02 and 0.2/0.02, the difference of current density was comparable to the transfer of the charge carriers for the oxidant-reductant electrolyte at 2/0.02 with respect to 0.2/0.02.

Key words: Oxidant-Reductant electrolyte, cadmium sulfide, Gerischer model, Indium tin oxide, ITO, ITO/CdS interface, Marcus.

INTRODUCTION

Cadmium sulfide which is abbreviated as CdS is a popular inorganic semiconductor that has been studied extensively for solar cells using chemical bath deposition method. It is also one of the most important groups of II–VI semiconductors with a band-gap of 2.4eV which is suitable for many other semiconductor device applications (Mahdi et al., 2012). This study chose CdS particularly because of its interesting behavior; due to its relatively high absorption coefficients, unique optical properties and ease to growth or deposit (Britt and Ferekides, 1993). CdS thin films have made a break-through in solar cells as a promising candidate for photovoltaic device especially those fabricated on indium tin oxide (ITO) substrates. Many material investigators have made a number of studies on nano-structured semiconductor electrodes (Ziabari and Ghodsi, 2012), but only a few have investigated the effect of a few redox electrolytes to improve the performance of research prototype solar cells. The most commonly investigated electrolyte is that of tri-iodide/ iodide (I_3^-/I^-) oxidant-reductant electrolyte couple but little has been done on

Fe^{+3}/ Fe^{+2} oxidant-reductant electrolyte system. Although, this tri-iodide/ iodide (I_3^-/I^-) oxidant-reductant electrolyte redox couple works efficiently in most materials tested, it has quite a number of disadvantages. It is important to study another redox couple and hence a choice was made on Fe^{+3}/ Fe^{+2} oxidant-reductant electrolyte system using Gerischer's approaches. In 1960, a researcher by the name Gerischer developed a solid-liquid model in which he postulated that charge transfer occur in terms of electronic energies in the solid and energy levels in solution associating it with those of ions (Ziabari and Ghodsi, 2012). This model later became suitable and can be applied when analyzing semiconductor electrodes because electron transfers occur through their conduction or valence bands. The work reported highlights theoretical approaches about effect of redox electrolytes in aqueous solvents on the photo-electrochemical behavior of CdS solar cells and demonstrates the behavior of Gerischer's model using CdS/ Fe^{+3}/ Fe^{+2} system. It also describes the interfacial electron transfer reactions using semi-classical theory between bands which was originally developed by Marcus for a donor-acceptor system in homogenous medium only.

THEORETICAL CONSIDERATIONS ON REDUCTION AND OXIDATION

The process of oxidizing involves the addition of oxygen to a compound with a loss of electrons and it is always accompanied by reduction. Any process in which electrons are added to an atom or ion (as by removing oxygen or adding hydrogen) is called reduction and is also always accompanied by oxidation of the reducing agent. Therefore, considering a simple redox reaction, the Nernst equation for a redox reaction in terms of electrochemical potentials is simplified so as to be expressed as:

$$\mu_{e,redox} = \mu^{\circ}_{e,redox} + kT \ln\left(\frac{C_{ox}}{C_{red}}\right) \quad (1)$$

where $\mu_{e,redox}$ is the electrochemical potential of electrons in the redox system; C_{ox} is the concentrations of the oxidation species and C_{red} is the concentrations of the reduction species. The electrochemical potential symbolized as $\mu_{e,redox}$ is equivalent to a Fermi level of a redox system, $E_{F,redox}$, The same test reference level is used for a solid electrode and any redox system as demonstrated in Equation 2 and Equation 1.

$$\mu_{e,redox} = E_{F,redox} \quad (2)$$

In most recent studies involving redox systems, corresponding redox potentials are given based on a natural conventional scale using the Ag/AgCl reference electrode (Xiao et al., 2012). Contrary to this approach, in the Gerischer model that is applied in this report, an electron transfer can occur from an occupied state in the metal or the semiconductor to an empty state in the redox system. This implies that in Gerischer model approach, the rate of electron transfer depends on the density of energy states on both sides of the interface irrespective of solid/liquid/electrolyte states. In a case where an electron transfer from the valence band of a semiconductor to the redox system occurs, the rate of transfer (Xiao et al., 2012) can be given by the expression as:

$$\mathrm{j}_v^- = \mathrm{e}\,\mathrm{k}_v^-\mathrm{N}_v\,\mathrm{C}_{ox} \quad (3)$$

where k_v^- is the rate constant in the valence band and N_v is the density of states in the valence band. This means that, if N_v is the approximate constant, then the ratio of j_v^- / C_{ox} as given in Equation 4 can be an appropriate criterion to use to manipulate the value of the rate constant in the valence band k_v^-:

$$\mathrm{j}_v^- / C_{ox} = \mathrm{e}\,\mathrm{k}_v^-\mathrm{N}_v \quad (4)$$

so as to obtain Equation 5. Therefore according to Equation 5, the value of k_v^- will be dependent on an exponential expression of redox Fermi ($E^{\circ}_{F,redox}$), the edge of the valence band at the semiconductor-electrolyte junction (E_v^s) and the re-orientation energy of redox (λ) respectively (Xiao et al., 2012). Thus using all this dependant parameters illustrated in Equation 5, the value of k_v^- as an exponential expression can be written as:

$$k_v^- = \mathrm{k}_0 - \exp\left(\frac{\left(E_v^s + \lambda - E^{\circ}_{F,redox}\right)^2}{4\mathrm{kT}\lambda}\right) \quad (5)$$

Using Equation 5, the accurate constant rate k_v^- as defined by Equation 5 can only be calculated if the values of λ and the energy difference $E_v^s - E^{\circ}_{F,redox}$ are known. However, if $E_v^s + \lambda = E^{\circ}_{F,redox}$ and is an exact value, then the value of constant k_v^- equals to maximum value of constant rate, k_0. This will estimate the value of k_v^- as a

constant and can be done by substituting j_v^- / C_{ox} from Equation 4 in Equation 5 and rearranging Equation 5 using Equations 6 and 7 as shown below taking the value of a as expressed in Equation 8 which will finally plot a curve of $\ln k_v^-$ versus $E^{\circ}_{F,redox}{}^2$ according to Equation 7.

$$\ln k_v^- = \ln k_0 - \frac{\left(E_v^s + \lambda - E^{\circ}_{F,redox}\right)^2}{4kT\lambda} \quad (6)$$

$$\ln k_v^- = -\frac{E^{\circ}_{F,redox}{}^2}{4kT\lambda} + a \quad (7)$$

The value of λ can thus be determined from slope. It found to be expressed from this line given from $[\frac{1}{4kT\lambda}]$ and hence the value of *a* can be expressed as:

$$a = \ln k_0 - \frac{(E_v^s + \lambda)^2 - 2(E_v^s + \lambda)E^{\circ}_{F,redox}}{4kT\lambda} \quad (8)$$

Many models (Xiao et al., 2012) approximate the value of $4kT\lambda$ to be about 0.1eV and this lets λ be easily calculated in the order of 1eV (Mahdi et al., 2012; Britt and Ferekides, 1993).

MATERIALS AND METHODS

Materials

Pyrex glass slides coated with ITO was used as a substrate. The following reagents and materials were used among others, $Cd(NO_3)_2$, thiourea, NaOH, $K_3Fe(CN)_6/K_4Fe(CN)_6$ all of analytical grade were bought from Merck Suppliers in Nairobi.

Preparations of solutions

Di-ionized water were used to prepare different concentrations of $K_3Fe(CN)_6/K_4Fe(CN)_6$ solutions as concentrations of Oxidation/Reductant electrolyte solutions. The prepared solutions were of different values of 0.02/0.02, 0.02/0.2, 0.2/0.02, 0.2/0.2 and 2/0.02 as required in set-up.

Cleaning of substrates

Pyrex glass slides coated with ITO were degreased in nitric acid for 24 h, washed with detergent, rinsed in di-ionized water and dried in air for 2 h (Mahdi et al., 2012; Britt and Ferekides, 1993). Pieces of the ITO substrate sheets with an area of 1 cm^2 were cut to be used, cleaned with distilled water, acetone and ethanol and finally ultra-sonicated in the isopropanol. They were kept for the Electro-deposition of CdS thin films.

Growth procedure

Preparation of ITO/CdS electrode

A solution of 0.1M $Cd(NO_3)_2$ was prepared to be used. CdS thin films were grown by electro-deposition on the indium tin oxide (ITO) to create the semiconductor solid. The redox solutions were used as the electrolytes for all other experimental tests. Sulfur was to be oxidized in the alkaline solution at about pH>10 from a solution containing 0.2 M thiourea. A few layers were grown and after electrodepositing of each layer, the surface of electrode was rinsed with distilled water to remove unabsorbed ions. The resulting electrode is denoted as ITO/CdS.

Preparation of redox solutions

Different concentrations of $K_3Fe(CN)_6/K_4Fe(CN)_6$ solutions as concentrations of Ox/Red solutions are as follows: 0.02/0.02, 0.02/0.2, 0.2/0.02, 0.2/0.2 and 2/0.02 and are shown in the Table 1.

Procedure for electro-deposition CdS thin films

Chronoamperometry is an electrochemical technique in which the potential of the working electrode is stepped and the resulting current from Faradaic processes occurring at the electrode is monitored as a function of time. Though limited information about the identity of the electrolyzed species can be obtained from the ratio of the peak oxidation current versus the peak reduction current, chronoamperometry generates high charging currents, which decay exponentially with time as any RC circuit. The Faradaic current is due to electron transfer events and decays as described in the Cottrell equation (Mahdi et al., 2012; Britt and Ferekides, 1993). Cottrell (1958) proposed an alternative dislocation mechanism for the nucleation of cleavage cracks in BCC metals such as ferritic iron. He argued that two dislocations slipping on intersecting (101) planes interact to form a new dislocation with Burgers vector normal to the cleavage plane. The interaction leads to a reduction in dislocation energy so that crack nucleation is easier than in the Zener-Stroh mechanism. Cottrell suggested that fracture by this mechanism would occur when the following criterion is met:

$$\sigma_f \geq \frac{2\mu\gamma}{k_y^s} d^{-1/2} \quad (9)$$

where d is the grain size, μ is the shear moduls, γ is the surface energy, and k_y is the Hall-Petch yielding constant

Table 1. Concentrations of $K_3Fe(CN)_6$/$K_4Fe(CN)_6$ solutions.

Redox agent	Concentrations of samples used				
	A	B	C	D	E
$K_3Fe(CN)_6$	0.02	0.02	0.2	0.2	2
$K_4Fe(CN)_6$	0.02	0.2	0.02	0.2	0.02

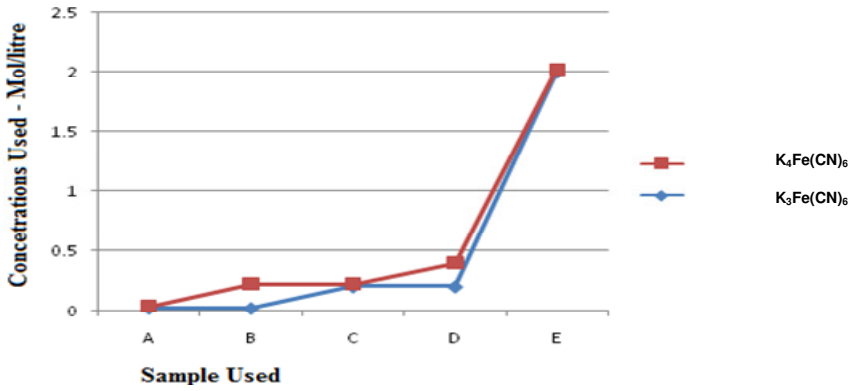

Figure 1. Relationship of the Ox/Red reagents and samples.

and this can apply to energy transitions in thin films. In most electrochemical cells, this decay is much slower than the charging decay and chronoamperometry gives a better signal to noise ratio in comparison to other amperometric technique (Mahdi et al., 2012; Britt and Ferekides, 1993). Chronoamperometry technique or method was used to electrodeposit the cadmium and sulfur for 1 min separately on the ITO substrates as follows: Firstly, Cd^{+2} were reduced on the ITO using in solution containing 0.1M $Cd(NO_3)_2$. Equally, sulfur was oxidized in these alkaline solutions at a pH>10 containing 0.2 M thiourea. After electrodepositing of each layer, the surface of electrode was rinsed with distilled water to remove unabsorbed ions. The resulting electrode is denoted as ITO/CdS. This UPD procedure was repeated 10 times to achieve 10 layers of CdS.

Techniques and instruments

Test instruments

All electrochemical measurements were carried out in a conventional three-electrode cell powered by a µ-Autolab-potentiostat/galvanostat and a frequency response analyzer at the University of Cape Town, at the School of Material Science laboratory.

Testing techniques

A frequency range of 100 kHz –10 MHz was used with modulation amplitude of 5 mV. This employed an Electrochemical Impedance spectroscopy (EIS). The impedance studies were carried out in open circuit potential (Ziabari and Ghodsi, 2012; Bashkirov et al., 2012; Repins et al., 2012) and later fitted in by Zview3.1 software. The Pyrex glass coated ITO was set as a working electrode while graphite was set as a counter. Finally, Ag/AgCl electrode was set as a reference electrode (Mahdi et al., 2012; Britt and Ferekides, 1993). A bulb of 100 W made from tungsten lamp was set as uniform light source.

RESULTS AND DISCUSSION

Figure 1 shows a plot of the relationship of the Ox/Red reagents used and labeled as sample A, B, C, and D in that order. The results obtained were expressed as curves obtained from the Zview3.1 software. Shown in Table 2 is the results of the simulation where *a,* is related to reduction of H_2O at -1.8V/Ag/AgCl.

It can be noted that from this table that from + 0.5 to -0.7V, the oxidation and reduction peaks plotted relates to the redox system of Fe^{+3} / Fe^{+2}. The curves in Figure 2 demonstrate the effect of the concentration of Fe^{+3} / Fe^{+2} redox system and how they affect the reduction peak current of Fe^{+3}, I_p. As it can be noted from the third column in Table 2, the highest reduction peak current is related to the redox electrolyte of Fe^{+3} / Fe^{+2} with 2/0.02 ratio as shown in Figure 2. The

Table 2. Kinetic constant rate from approximated relation by substituting j_v^- / C_{ox} instead of k_v^-

Ox / Red (M)	$E_{F,redox}$ (V)	I_p (A) x 10^4	$E^{\circ}_{F,redox}{}^2$	$1_{j_v^-}$ (A)	$1_{j_v^-}/_{Cex}$	$\frac{1}{\ln k_v^-}$
0.02/0.02	+0.58	6.93	0.49	-0.013	0.65	-0.43
0.02/0.2	+0.52	23.5	0.59	-0.012	0.6	-0.51
0.2/0.02	+0.64	7.7	0.68	-0.017	0.085	-2.46
0.2/0.2	+0.58	20	0.49	-0.021	0.105	-2.25
2/0.02	+0.74	50	0.77	-0.026	0.013	-4.34

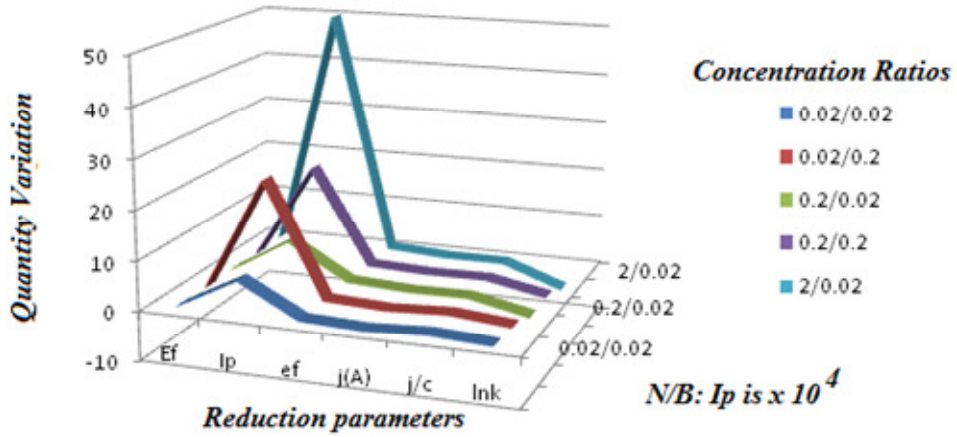

Figure 2. Plot of concentration and reduction parameters.

simultaneous increase in the values of $E_{F,redox}$ and their corresponding Fe^{+3} concentrations confirm the positive effect and effectively increases the value of the current I_p. Another cathodic current initiated at -0.7V/Ag/AgCl as a reference electrode continues to increase up to the more negative potentials. These negative potentials are related to the reduction of H_2O (Xiao et al., 2012) and this implies that the reduction of Fe^{+3} simultaneously accompanies the reduction of water in this same region because the reduction of current increases as Fe^{+3} concentration increases.

This reduction observed on the CdS thin film surface can be reasoned from the CdS thin film band structure (Mahdi et al., 2012; Britt and Ferekides, 1993) and how it interacts with the potential of Fe^{+3}/Fe^{+2} redox agent. Therefore, to analyze these curves, the position of the energy bands at the surface of CdS thin films in aqueous solutions must be taken into account (Mahdi et al., 2012). This approach confirms the references obtained in the valence and conduction band position in CdS in the dark are placed at +0.7 and -1.7V/Ag/AgCl, respectively (Ziabari and Ghodsi, 2012; Bashkirov et al., 2012; Repins et al., 2012) and the electrochemical standard potential of Fe^{+3}/Fe^{+2} obtained was 0.58V/Ag/AgCl. Figure 2 and Table 2 concurrently show that the reduction of Fe^{+3} ions is initiated at +0.5V/Ag/AgCl and therefore accordingly, the valence band position of CdS at + 0.7V/Ag/AgCl, and the reduction current of Fe^{+3} when compared, occur in the valence band of CdS due to vicinity of energy levels. It was also observed that by increasing of the concentration of the oxidized species (Fe^{+3}) from 0.02 to 2 Molar, the values of $E_{F,redox}$ changes from 0.58 to 0.74V/Ag/AgCl respectively and result into a redox Fermi level of Fe^{+3}/Fe^{+2} which equally approximates to the theoretical energy level of CdS valence band which causes a reduction current in this region.

A similar observation (Mahdi et al., 2012; Britt and Ferekides 1993) has been obtained for H_2O though lower. Increasing the oxidized species (Fe^{+3}) from 0.02 to 2 changes the value of $E_{F,redox}$ from 0.58 to 0.74V/Ag/AgCl reference electrode. This causes the reduction current of H_2O from -0.013 to -0.026A at -1.8V/Ag/AgCl respectively (Ziabari and Ghodsi, 2012; Bashkirov et al., 2012; Repins et al., 2012) and this change results into a change of $\ln k_v^-$ from -0.43 to - 4.34 which implies that the rate constant is reduced or

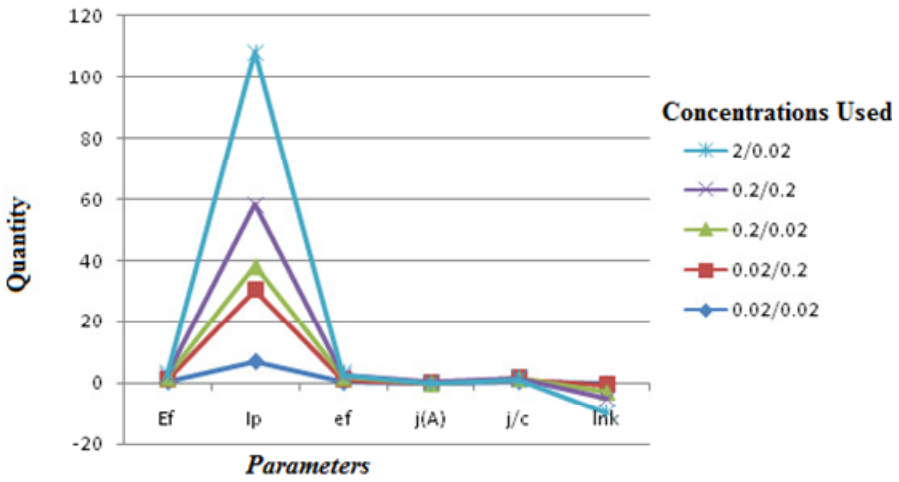

Figure 3. CdS thin film at the OCP under dark and light conditions for the two concentrations of redox electrolyte.

decreased. When the concentration of oxidized species increases, $E^{\circ}_{F,redox}{}^{2}$ increase too and the kinetic constant rate decreases inversely. This is in good agreement with Equation 7 that increase of $E^{\circ}_{F,redox}{}^{2}$ causes decrease of the $\ln k_v^-$ because of negative sign of $E^{\circ}_{F,redox}{}^{2} / 4kT\lambda$. The re-orientation energy of redox (λ) from slope of this line is obtained as 0.7eV. This value is within the acceptable limits of Gerischer model. Using the theoretical approach (Ziabari and Ghodsi, 2012; Bashkirov et al., 2012; Repins et al., 2012) and current difference demonestrated in out theory part 2.0 and an applied potential in the dark and light conditions, a lot of concern can be raised to the light induced processes (Mahdi et al., 2012). Under applied overvoltages and in the dark, the cathodic current follow Equation 9 and using j_0 as an exchange current, j_v^- can then be expressed as:

$$j_v^- = -j_0[\exp(-\frac{e\eta}{kT}) - 1] \quad (9)$$

It is therefore noted that the value of j_v^- in the dark condition is only dependent on applied overvoltage which can be symbolized as, η. According to the plot shown in Figure 2, the value of j_v^- at 0.0V/Ag/AgCl reference electrode in the dark and light conditions imply effective higher light induced current. This unique phenomenon demonstrates and equally admits the existence of a relationship between the Fermi Redox Energy and Band Energy position (Shah et al., 2012; Xiao et al., 2012; Nyquist and Kagel, 2012) especially in CdS tested in this work. A Nyquist spectra plot (Nyquist and Kagel, 2012) can equally be plotted so that that curve will show the relationship of CdS thin film at the OCP in the dark and under light conditions for the used concentrations of redox electrolytes. The highest values of j_v^- will be demonstrated by Figure 3. This work can also use spectra fitted into Randles equivalent circuit and it will show a high frequency region, in which the value of R_s would be related to the resistance of the CdS thin film in different concentrations of redox electrolyte. A Randles circuit is an equivalent electrical circuit that consists of an active electrolyte resistance R_S in series with the parallel combination of the double-layer capacitance C_{dl} and an impedance of a faradaic reaction. It is commonly used in Electrochemical impedance spectroscopy (EIS) for interpretation of impedance spectra, often with a Constant phase element (CPE) replacing the double layer capacity (C_{dl}).

Figure 4 shows the equivalent circuit initially proposed by John Edward Brough Randles for modeling of interfacial electrochemical reactions in presence of semi-infinite linear diffusion of electroactive particles to flat electrodes. In this model, the impedance of a Faradaic reaction consists of an active charge transfer resistance R_{ct} and a specific electrochemical element of diffusion W, which is also called Warburg element ($Z_W = A_W/(j\omega)^{0.5}$, where A_W is Warburg coefficient, j – imaginary unit, ω – angular frequency). Figure 5 shows an example of EIS spectrum (presented in the Nyquist plot) simulated using the following parameters: R_S = 20 Ω, C_{dl} = 25 μF, R_{ct} = 100 Ω, A_W = 300 Ω•$s^{-0.5}$.

In a simple situation, the Warburg element manifests itself in EIS spectra by a line with an angle of 45° in the low frequency region. Values of the charge transfer resistance and Warburg coefficient depend on physico-chemical parameters of a system under investigation. To obtain the Randles circuit parameters, the fitting of the

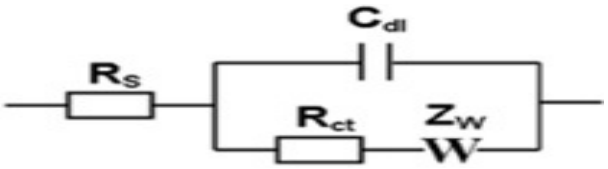

Figure 4. Randles equivalent circuit.

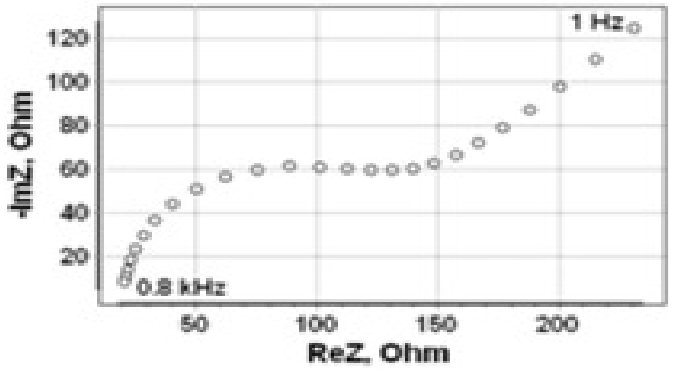

Figure 5. Simulated EIS spectrum of the Randles circuit.

model to the experimental data should be performed using complex nonlinear least-squares procedures available in numerous EIS data fitting computer programs. The Randles equivalent circuit is one of the simplest possible models describing processes at the electrochemical interface. In real electrochemical systems, impedance spectra are usually more complicated and, thus, the Randles circuit may not give appropriate results. When calculated, the diameter of semicircle (R_{ct}) was found to be related to resistance of charge carriers in CdS semiconductor. The decrease in value of R_{ct} at light condition (*not shown in any of the curves or figure in this report*) was due to the increase of the charge carriers such as electron in n-type semiconductors present in CdS thin films (Shah et al., 2012; Xiao et al., 2012; Nyquist and Kagel, 2012).

This demonstrated that the difference of the current density was comparable to the transfer of the charge carrier for redox electrolyte. This was confirmed from the difference of R_{ct} values on the I-V plots and the value of the charge transfer resistance is therefore related to the current density j_v^- reversely (*not shown in any of the curves or figure in this report*). The value of R_{ct} in the redox electrolyte 2/0.02 was obtained to be near its value in the redox electrolyte 0.2/0.02 when the CdS thin film was in darkness. The values of R_{ct} differ remarkably when under illumination and can be plotted in Bode phase plots which may also show a positive relationship if Nyquist plots in different concentrations of redox electrolyte are plotted.

Conclusion

A study was conducted to demonstrate the electron transfer between electrolytes and a semiconductor of CdS. Chronoamperometry technique was employed to electrodeposit cadmium and sulfur separately on ITO to form ITO/CdS as a semiconductor interface and was tested against the ITO/CdS/$K_3Fe(CN)_6$/$K_4Fe(CN)_6$ interface. The CV measurements of the ITO/CdS in the redox electrolyte with different concentration of Fe^{+3}/Fe^{+2} was done and showed that the highest reduction current was related to the redox electrolyte of Fe^{+3}/Fe^{+2} with 2/0.02 ration and $E_{F,redox}$ = 0.74eV. The valence band position of CdS and the reduction current of Fe^{+3} were found to occur in the valence band. Experiment showed that when concentration of oxidized species and $E^{\circ}_{F,redox}{}^{2}$ increase, the kinetic constant rate decreases inversely. EIS studies showed that the difference of the current density was comparable to transfer of the charge carrier for redox electrolyte 2/0.02 with respect to 0.2/0.02. It was concluded that manipulating CdS/Fe^{+3}/Fe^{+2} can improve and optimize the design of CdS thin film solar interface.

ACKNOWLEDGEMENTS

The authors are gratefully acknowledging Technical University of Mombasa for providing financial support to

facilitate Electrochemical Impedance spectroscopy tests (EIS), University of Nairobi for allowing the authors to use their test instruments, the Physics laboratory technicians of Maasai Mara University and Kenyatta University for providing the simulation software.

REFERENCES

Bashkirov SA, Gremenok VF, Ivanov VA, Lazenka VV, Bente K (2012). Tin sulfide thin films and Mo/p-SnS/n-CdS/ZnO heterojunctions for photovoltaic applications. Thin Solid Films 520(17):5807-5810.

Britt J, Ferekides C (1993). Thin-film CdS/CdTe solar cell with 15.8% efficiency. Appl. Phys. Lett. 62(22):2851-2852.

Mahdi MA, Hassan Z, Ng SS, Hassan JJ, Bakhori SM (2012). Structural and optical properties of nanocrystalline CdS thin films prepared using microwave-assisted chemical bath deposition. Thin Solid Films 520(9):3477-3484.

Meshram RS, Suryavanshi BM, Thombre RM (2012). Structural and optical properties of CdS thin films obtained by spray pyrolysis. Adv. Appl. Sci. Res. 3:1563-1571.

Nyquist RA, Kagel RO (2012). Handbook of infrared and raman spectra of inorganic compounds and organic salts: infrared spectra of inorganic compounds (Vol. 4). Academic press.

Repins I, Beall C, Vora N, DeHart C, Kuciauskas D, Dippo P, ... Noufi R (2012). Co-evaporated Cu 2 ZnSnSe 4 films and devices. Sol. Energy Mater. Sol. Cells 101:154-159.

Shah NA, Nazir A, Mahmood W, Syed WAA, Butt S, Ali Z, Maqsood A (2012). Physical properties and characterization of Ag doped CdS thin films. J. Alloys Compd. 512(1):27-32.

Xiao L, Damien J, Luo J, Jang HD, Huang J, He Z (2012). Crumpled graphene particles for microbial fuel cell electrodes. J. Power Sources 208:187-192.

Ziabari AA, Ghodsi FE (2012). Growth, characterization and studying of sol–gel derived CdS nanoscrystalline thin films incorporated in polyethyleneglycol: effects of post-heat treatment. Sol. Energy Mater. Sol. Cells 105:249-262.